Two-photon double ionization of helium by chirped few-cycle attosecond pulses: From nonsequential to sequential regime*

Yao Tong(童瑶)[1], Wei-Chao Jiang(姜维超)[1,2], Pan Wu(伍攀)[1], and Liang-You Peng(彭良友)[1,3,†]

[1] *State Key Laboratory for Mesoscopic Physics and Collaborative Innovation Center of Quantum Matter, School of Physics, Peking University, Beijing* 100871, *China*

[2] *Institute for Theoretical Physics, Vienna University of Technology, Wiedner Hauptstraße* 8-10, *A*-1040 *Vienna, Austria*

[3] *Collaborative Innovation Center of Extreme Optics, Shanxi University, Taiyuan* 030006, *China*

(Received 26 February 2016; revised manuscript received 9 May 2016; published online 1 June 2016)

The two-photon double ionization (TPDI) dynamics of helium by chirped attosecond pulses are theoretically studied by solving the two-electron time-dependent Schrödinger equation in its full dimensions. We show that both the differential and the total double ionization probability can be significantly controlled by adjusting the chirp. The dependence of the TPDI on the chirp can be quite different for different photon energies, relying on the central photon energy being in the sequential region, nonsequential region, or translation region. The physics which lead to the chirp dependence for different photon energies are addressed. Present findings are well reproduced by a model based on the second-order time-dependent perturbation theory.

Keywords: time-dependent Schrödinger equation (TDSE), double ionization, electron correlation, chirp

PACS: 32.80.Rm, 42.50.Hz, 42.65.Re **DOI:** 10.1088/1674-1056/25/7/073202

1. Introduction

Laser sources[1,2] in a wide range of frequency have enabled the observation and control of the internal atomic and molecular dynamics on its natural time scale.[3–7] The actual control of these dynamics is realized through the change of parameters of one or multiple laser pulses, and the chirp of the pulse is among the many parameters which one can play with.[8] In the infrared range, technologies of precise control of the chirp of a laser pulse have been rather mature and thus the chirp parameter has been utilized to control many physical processes, such as the excitation dynamics of molecular vibrational and rotational states (see, e.g., Refs. [9]–[14]) and the population transfer in few-level model atoms,[15–18] the extension of the plateau cutoffs for both the high-order harmonic generation (HHG)[19–24] and the above threshold ionization (ATI),[25–29] the production of a single attosecond pulse,[30] the ultracold atomic collisions,[31] etc.

In the extreme ultraviolet (xuv) regime, few-cycle and single-cycle[32–34] single attosecond pulses with a stable and even tunable carrier envelope phase (CEP) have been achieved experimentally. Significant effects of the CEP on ionized electron momentum and energy distributions have been investigated theoretically in some detail.[35–38] It is well known that current technologies for generating attosecond pulses based on the HHG introduce an inherent chirp[39] in the xuv regime. A few years ago, the first experimental demonstration[40] was reported to effectively control the frequency chirp of isolated attosecond xuv pulses by aperiodic multilayer mirrors, which promises that it is possible to engineer the frequency dispersion of attosecond pulses in a wide range of xuv photon energies and bandwidths. Based on these experimental advances in xuv chirping technologies, it is important to look at the effects of the chirp on the ionization dynamics in the xuv region.

For single ionization dynamics, the chirp effects have been extensively explored. It has been shown that the chirped attosecond pulses can measure attosecond time scale electron dynamics just as effectively as transform-limited attosecond pulses of the same bandwidth.[41] However, the chip of the pulses can also produce significant effects on the ionization signal,[42,43] thus providing another way to control electron dynamics. Experimentally, the introduction of the chirp changes the coming order of a particular frequency, but the spectrum profile (frequency spectrum) of the pulse is conservative. So the chirp does not produce any effect on the one-photon ionization dynamics, since the amplitude of one-photon ionization is simply proportional to the spectrum profile of the pulse. However, for nonlinear ionization dynamics, the chirp can have significant effects. The dependence of atomic ionization dynamics on the chirp of a few-cycle attosecond pulse has been thoroughly investigated by different theoretical methods.[44–46]

The double ionization dynamics turns out to be a much more challenging problem than the single ionization dynamics, both experimentally and theoretically. The most fundamental nonlinear double ionization dynamics is the two-

*Project supported by the National Natural Science Foundation of China (Grant Nos. 11322437 and 11574010) and the National Basic Research Project of China (Grant No. 2013CB922402).

†Corresponding author. E-mail: liangyou.peng@pku.edu.cn

© 2016 Chinese Physical Society and IOP Publishing Ltd

photon double ionization (TPDI) of helium, which has attracted a lot of experimental[47,48] and theoretical attentions (see, e.g., Ref. [5], [49]– [51] and references therein). One of the emphasises of these studies has been focused on the sequential and nonsequential picture of the TPDI and the role of the electron–electron correlation played in the differential and total double ionization cross section. Recently, the chirp effects for the TPDI of helium have also been predicted by several calculations. Double ionization of the He atom by a chirped attosecond XUV pulse of central photon energy 91.6 eV was investigated[52] by solving the two-electron time-dependent Schrödinger equation (TDSE), it was found that the single and double electron energy spectra are quite sensitive to the pulse chirp in this deep sequential regime. Last year, an effective control of the double ionization probability was numerically demonstrated for a central photon energy of 52.7 eV,[53] which is very close to the second ionization threshold of helium. To the best of our knowledge, such a chirp-dependence study in the nonsequential region has not been carried out.

In the present work, we revisit the chirp dependence of TPDI of helium by a few-cycle attosecond pulses in a wide range of central photon energies from the nonsequential to the sequential regime. Our studies are carried out by two different methods, i.e., the *ab initio* solution to the two-electron TDSE[54,55] and a model based on the second-order time-dependent perturbation theory (TDPT).[50,56] From the comparison studies at different photon energies from both methods, we find that the chirp-dependence of the double ionization dynamics is drastically different in different regions, relying on that the central photon energy is in the sequential region, nonsequential region, or translation region. These differences manifest in both the differential and integral ionization probabilities.

In the rest of the paper, we first briefly revisit our numerical methods of TDSE and TDPT. Then we will present our results for the total ionization probability as a function of the chirp of the pulse, followed by the joint differential energy distributions of the two electrons at selected values of the pulse chirp at three different photon energies, respectively corresponding to the nonsequential, sequential, and the transition across the second ionization threshold. We find clearly different chirp dependence in different regions. Finally, we make a brief summary for present work. Atomic units ($m_e = h = e = 1$) are used throughout the paper unless otherwise stated.

2. Theoretical methods

We solve the time-dependent Schrödinger equation in its full dimensionality. The details of the numerical technologies can be found in our previous work.[5,51,54] The TDSE of helium in a linearly polarized laser field is given by

$$\mathrm{i}\frac{\partial}{\partial t}\Psi(\boldsymbol{r}_1,\boldsymbol{r}_2,t) = H(t)\Psi(\boldsymbol{r}_1,\boldsymbol{r}_2,t), \tag{1}$$

where the Hamiltonian operator, in the dipole approximation and length gauge, can be written as

$$\begin{aligned} &H(\boldsymbol{r}_1,\boldsymbol{r}_2,t) \\ &= \frac{\boldsymbol{p}_1^2}{2} + \frac{\boldsymbol{p}_2^2}{2} - \frac{2}{r_1} - \frac{2}{r_2} + \frac{1}{|\boldsymbol{r}_1-\boldsymbol{r}_2|} + (\boldsymbol{r}_1+\boldsymbol{r}_2)\cdot\boldsymbol{E}(t), \end{aligned} \tag{2}$$

where $\boldsymbol{E}(t)$ is the electric field of the laser pulse, related to the vector potential of the pulse through

$$\boldsymbol{E}(t) = -\frac{\partial \boldsymbol{A}(t)}{\partial t}. \tag{3}$$

For the purposes of the present study, we adopt a chirped attosecond laser pulse having a Gaussian form.[26,44] The vector potential of the linearly polarized laser pulse along the z axis is given by

$$\boldsymbol{A}(t) = A(\xi)F(t)\sin[\omega(t)t]\,\boldsymbol{e}_z, \tag{4}$$

where ξ is the chirp of the pulse. The chirp-dependent peak amplitude $A(\xi)$, chirped carrier frequency $\omega(t)$, and time envelope $F(t)$ are given respectively by

$$A(\xi) = \frac{E(\xi)}{\omega_0} = \frac{1}{\omega_0}\sqrt{\frac{I_0/I_{\mathrm{au}}}{\sqrt{1+\xi^2}}}, \tag{5}$$

$$\omega(t) = \omega_0 + 2\ln 2\frac{\xi}{1+\xi^2}\frac{t}{\tau_0^2}, \tag{6}$$

$$F(t) = \exp\left[-2\ln 2\frac{1}{1+\xi^2}\frac{t^2}{\tau_0^2}\right], \tag{7}$$

in which $I_{\mathrm{au}} = 3.51\times10^{16}$ W/cm^2 is the atomic unit of intensity. The case $\xi = 0$ corresponds to a Fourier transform-limited pulse with carrier frequency ω_0, peak intensity I_0, and pulse duration τ_0 (full width at half maximum, FWHM). For a chirped pulse, the peak intensity and pulse duration are given respectively by $I_{\xi 0} = I_0/\sqrt{1+\xi^2}$ and $\tau_{\xi 0} = \tau_0\sqrt{1+\xi^2}$. The optical period corresponding to the central carrier frequency ω_0 is defined as $T_0 = 2\pi/\omega_0$. As an example, we compare in Fig. 1 the vector potential for an unchirped pulse with those having a zero, positive and a negative chirp for $\tau_0 = 460$ as and $\omega_0 = 52.4$ eV.

The vector potential (4) simulates a realistic experimental case in which a nonzero chirp ξ leads to an increase of the pulse duration and a decrease of the pulse intensity for a fixed total pulse energy. The spectrum profile (or frequency spectrum) of the chirped pulse defined by Eqs. (4), (5), and (7) does not depend on the chirp, i.e., all the spectrum profiles of the chirped pulses remain the same as the tranform-limited case. We notice that in the recent study,[53] the definition of the chirped pulses does not make sure the spectrum profile is

independent on the chirp, though in a related work about H atom[57] by the same authors exactly the same definition for the chirped pulses with the present work is taken. It is in fact our initial motivation to see how a more physical definition for the chirp pulse will influence the conclusion of Ref. [53].

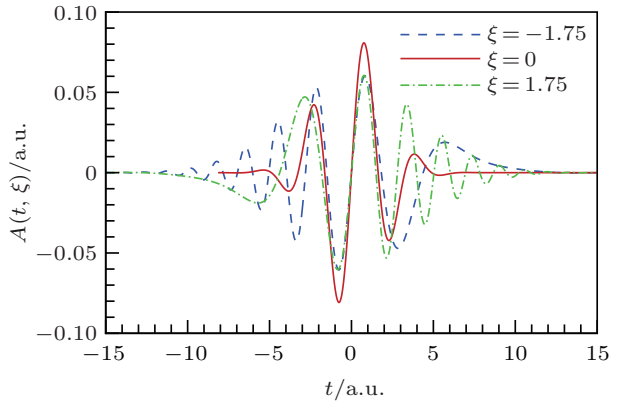


Fig. 1. (color online) The vector potentials of the laser pulses for $\xi=0$ and ±1.75. In this example, we take the central frequency $\omega_0=52.4$ eV, the peak intensity $I_0=1\times10^{15}$ W/cm^2, and $\tau_0=460$ as.

After the numerical solution to Eq. (1), one can evaluate the fully differential double ionization probability by projecting the final wave function onto the product of two scattering states of hydrogen-like atom with a nuclear charge of 2. Please note, after the end of the laser pulse, the final wave function is freely propagated for a sufficiently long time to make this extraction method reliable. Integrating the fully differential double ionization probability over ejection angles of the two electrons can give us the joint energy spectra

$$P(E_1,E_2)=\frac{1}{k_1k_2}\iint P(\boldsymbol{k}_1,\boldsymbol{k}_2)k_1^2k_2^2\,\mathrm{d}\hat{k}_1\,\mathrm{d}\hat{k}_2, \tag{8}$$

where $P(\boldsymbol{k}_1,\boldsymbol{k}_2)$ is the fully differential double ionization probability. The total double ionization probability is obtained by carrying out the integration

$$P_{\mathrm{total}}=\iint P(E_1,E_2)\,\mathrm{d}E_1\,\mathrm{d}E_2. \tag{9}$$

The same quantities $P(E_1,E_2)$ and P_{total} can also be calculated by the TDPT, which has shown its accuracy and transparency in recent studies.[50,56,58] In this analytical and semi-quantitative TDPT calculation, the joint energy spectra of the two electrons can be given by

$$P(E_1,E_2)=\frac{1}{2}\left(\frac{c}{4\pi^2}\right)^2\left|\sqrt{\frac{\sigma^{\mathrm{He}}(E_1)}{\omega_{\mathrm{ai}}}}\sqrt{\frac{\sigma^{\mathrm{He^+}}(E_2)}{\omega_{\mathrm{fa}}}}K(E_{\mathrm{a}})+\sqrt{\frac{\sigma^{\mathrm{He}}(E_2)}{\omega_{\mathrm{bi}}}}\sqrt{\frac{\sigma^{\mathrm{He^+}}(E_1)}{\omega_{\mathrm{fb}}}}K(E_{\mathrm{b}})\right|^2, \tag{10}$$

where c is the speed of light, $E_{\mathrm{a}}=E_1+E_0$, $E_{\mathrm{b}}=E_2+E_0$, $E_0=-54.4$ eV is the ground state energy of $\mathrm{He^+}$, $\omega_{\mathrm{ai}}=E_{\mathrm{a}}-E_{\mathrm{i}}$, $\omega_{\mathrm{fa}}=E_{\mathrm{f}}-E_{\mathrm{a}}$, and $E_{\mathrm{i}}=79.0$ eV is the ground state energy of helium, σ^{He} and $\sigma^{\mathrm{He^+}}$ are respectively the one-photon single ionization cross section of He and $\mathrm{He^+}$,[59] and $K(E_{\mathrm{a}})$ stands for a double integration over the electric field

$$K(E_{\mathrm{a}})=\int_{-\infty}^{\infty}\mathrm{d}\tau_1E(\tau_1)\,\mathrm{e}^{\mathrm{i}\omega_{\mathrm{fa}}\tau_1}\int_{-\infty}^{\tau_1}\mathrm{d}\tau_2E(\tau_2)\,\mathrm{e}^{\mathrm{i}\omega_{\mathrm{ai}}\tau_2}, \tag{11}$$

where $E(t)=|\boldsymbol{E}(t)|$ is the electric field of the pulse. The total ionization probability P_{total} from the prediction of the TDPT can then be evaluated through Eq. (9).

3. Results and discussion

As mentioned in the Introduction, the two-photon double ionization of helium shows different features for different central photon energies. For the case of few-cycle attosecond pulses, the chirp of the pulse will significantly change the appearing time sequence of different frequency components contained in the pulse, as shown in Fig. 1. Therefore, it is expected that, the TPDI dynamics will depend on the change of the chirp. These differences may manifest in either the differential ionization probability, or the total TPDI yield, or both, depending on the central photon energy.

In this section, we will systematically investigate the critical dependence of the TPDI on the chirp of the few-cycle attosecond pulses. For these purposes, we fix the peak intensity I_0 of the transform-limited pulse to be at 1×10^{15} W/cm^2 and change the central photon energy ω_0 and the chirp parameter ξ. Please recall that, the effective peak intensity and pulse duration will depend on ξ in such a way that the total energy and the spectrum profile of the chirped pulses will stay the same with the corresponding transform-limited case.

First, let us focus on the dependence of the total ionization yield on the chirp of the pulse. What shown in Fig. 2 are the total TPDI probability P_{total} as a function of the chirp parameter ξ, varying from -2 to 2. The results are shown for four different central photon energies ω_0, i.e., (a) 45 eV, (b) 52.4 eV, (c) 60 eV, and (d) 70 eV. In all these calculations, the number of cycles for each ω_0 is fixed to be 6, i.e., $\tau_0=6T_0$. One notices that the results from TDSE and from TDPT agree with each other rather well for all the cases. In TDSE calculation, not only the contribution from the second-order perturbation but also the contributions from the first- and third-order perturbations are counted. This would explain the small differences between the results of TDSE and TDPT in Fig. 2.

When $\omega_0=45$ eV in the nonsequential TPDI regime, as can be seen from Fig. 2(a), the total yield decreases with the increase of the absolute value of the chirp parameter and does not depend on the sign of the chirp (i.e., the curve is symmetric about $\xi=0$). This can be understood as follows. For nonsequential TPDI around $\omega_0=45$ eV, the total cross section σ does not significantly change as photon energy ω_0. So the dependence of the total double ionization probability P_{total} on the chirp ξ would roughly be

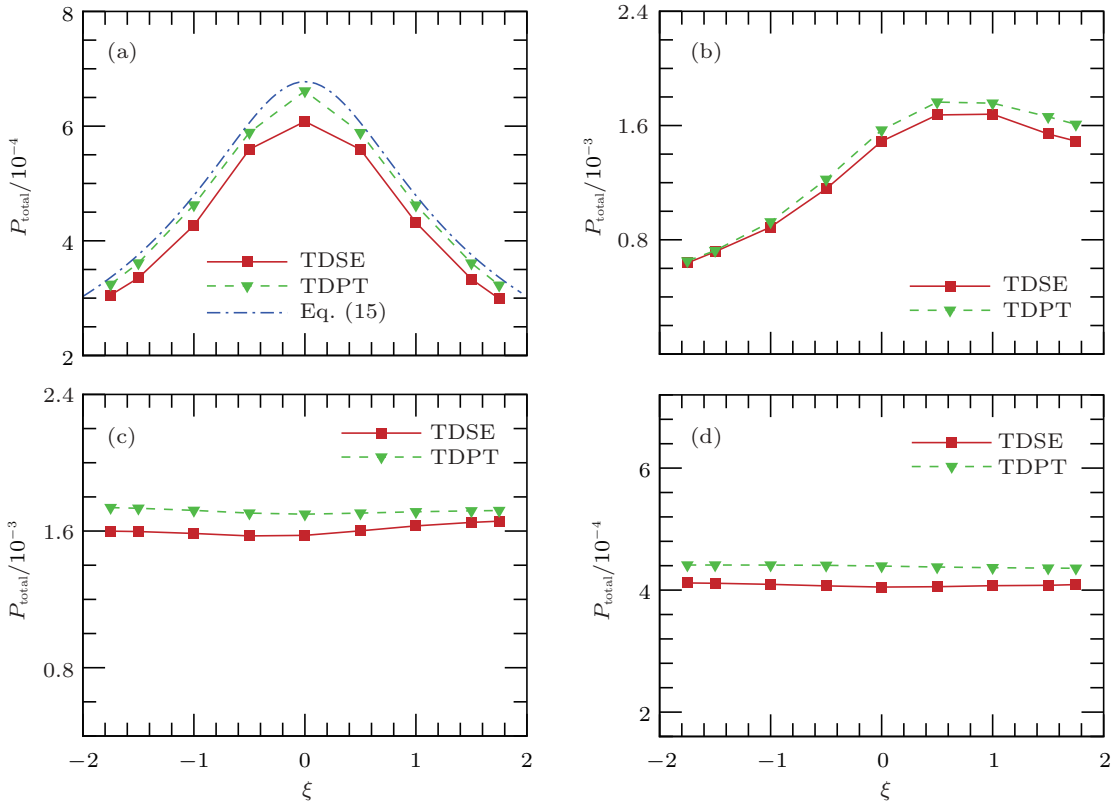


Fig. 2. (color online) Total two-photon double-ionization probability $P_{\rm total}$ as a function of the chirp parameter ξ, respectively, calculated by TDSE (squares) and by TDPT (triangles), for four different central photon energies ω_0: (a) 45 eV, (b) 52.4 eV, (c) 60 eV, and (d) 70 eV.

$$P_{\rm total} = \sigma \frac{I_{\xi 0}^2}{\omega_0^2} T_{\xi \rm eff}, \tag{12}$$

where

$$I_{\xi 0} = I_0/\sqrt{1+\xi^2}, \tag{13}$$

$$T_{\xi \rm eff} = \sqrt{\frac{\pi}{16\ln 2}}\tau_0\sqrt{1+\xi^2}. \tag{14}$$

Putting Eqs. (13) and (14) into Eqs. (12), one obtains

$$P_{\rm total} = \sqrt{\frac{\pi}{16\ln 2}}\sigma\frac{I_0^2}{\omega_0^2}\tau_0\frac{1}{\sqrt{1+\xi^2}}. \tag{15}$$

Predictions from Eqs. (15) ($\sigma = 1.2\times10^{-52}$ cm^4 is taken from Ref. [50]) are also shown by the dash-dotted line in Fig. 2(a).

In Fig. 2(b), ω_0 is increased to 52.4 eV, which is about 2 eV smaller than the second ionization threshold of helium. One observes that the trend of the total yield curve is drastically different from that in Fig. 2(a). The main difference is that the curve is no longer symmetric about ξ and the total yield is continually increased as ξ is increased from -1.75 to 1.75 with a kind of saturation at the end of the positive chirp. The same observation was recently discussed by Barmaki and coworkers[53] at a slightly higher ω_0 of 52.7 eV. The total yield dependence on ξ for this case of ω_0 is closely related to the fact that the frequency components cover the whole transition region from the nonsequential to the sequential TPDI process so that the two electrons get ionized in two different ways. This will lead to different effects for down-chirped ($\xi < 0$) and up-chirped ($\xi > 0$) pulses. For the case of $\xi < 0$, the higher frequency components come first and the lower ones come last. Thus, for a significant range of time period in the latter half of the chirped pulse, the effective photon frequency will be smaller than 54.4 eV, the TPDI will happen in the nonsequential region, with its probability proportional to the effective duration in this region. In this case, the sequential ionization channel with the first electron absorbing a smaller photon and the second electron a larger photon will be largely suppressed. Such a process is only possible for a restricted effective time period in the earlier half of the pulse. On the contrary, for the case of $\xi > 0$, the lower frequency components come first and the higher ones come last, which will leave the above mentioned channel of sequential ionization open for almost all the pulse duration. If one bears in mind that the total yields of the sequential TPDI is much higher than the nonseqential TPDI and the ionization yield of the sequential TPDI is proportional to the square of the effective pulse duration,[50] it is immediately understood why the total TPDI yield of $\xi = 1.75$ is more than 3 times of that for $\xi = -1.75$. In addition, as analyzed in Ref. [53], there is a possibility of populating the Rydberg series of He^+, which may also contribute to the strong chirp dependence observed for the case of the central photon energy close to the second ionization threshold.

When one continues to increase ω_0 to 60 eV, which is above the second ionization threshold of helium. The TPDI will dominantly happen in a sequential fashion. Since the dependence of the total double ionization on the peak intensity and pulse duration is on the same power,[50] i.e., $P_{\rm total} \propto (I_{\xi 0}/\tau_{\xi 0})^2$, one expects that the total yield will not critically depend on the chirp of the pulse. What is shown in Fig. 2(c) is indeed a rather flat curve, with a slight increase when the chirp is increased. This small increase is simply because for such a short pulse considered here, there is still a small fraction of the frequency components that falls below 54.4 eV. Therefore, the mechanism explained above may still play a minor role. However, when ω_0 increases to 70 eV in Fig. 2(d), which is well above 54.4 eV, we observe a much flatter curve and the dependence of $P_{\rm total}$ on the chirp parameter ξ is almost negligible.

For a better intuitive understanding of the total TPDI yield as a function of the central photon energy ω_0 and the chirp parameter ξ, as discussed above, it is instructive to examine the differential ionization probability. We first focus on the angle-integrated joint energy distributions of two electrons, i.e., $P(E_1, E_2)$. The evolutions of the density distribution for three different chirp parameters are respectively shown in Fig. 3 for $\omega_0 = 45$ eV, in Fig. 4 for $\omega_0 = 54.2$ eV, and in Fig. 5 for $\omega_0 = 70$ eV. In each of these three figures, the results calculated by TDSE are presented in the first row, and those evaluated from the TDPT model are shown in the second row. Please note that each column in each figure shares the same contour color scheme. As we can see, our results from both methods agree very well with each other quantitatively. It is not surprising, as demonstrated in previous studies,[50,56,58] the TDPT model can not only reproduce the total ionization yield, but also give the correct angle-integrated joint energy distributions.

Let us first look at the case of $\omega_0 = 45$ eV, shown in Fig. 3. In this nonsequential regime, we can see that the shape of the differential ionization probability looks similar due to the unchanged frequency components. We thus use the same color bar for all the six panels. Compared to the case of $\xi = 0$, the reason that the differential probability is lower for $\xi = \pm 1.75$ can be easily understood from the fact that the nonsequential double ionization is proportional to $I_{\xi 0}^2 T_{\xi \rm eff} \propto 1/\sqrt{1+\xi^2}$, as discussed above by the perturbation model.

When ω_0 is increased to the crossover case of 52.4 eV for the nonsequential and sequential regime, one can notice that the gross feature in Fig. 4 is the sequential peaks of the ejected electrons. However, for $\xi = -1.75$ and 0, there are unnegligible signals for the equal energy sharing case. Another noticeable feature is that, the electrons for $\xi = -1.75$ have a wider spectra than those for $\xi = 0$ and $\xi = 1.75$. This is due to the fact that the double ionization for $\xi = -1.75$ is confined to a narrower time window than those of the latter two cases, which results in a wider electron spectra. The case of $\xi = 1.75$ becomes more sequential-type because in this case, the sequential TPDI channel is open for most of the effective pulse duration, in which case the atom first absorbs a photon with a smaller energy and then a photon with a larger energy.

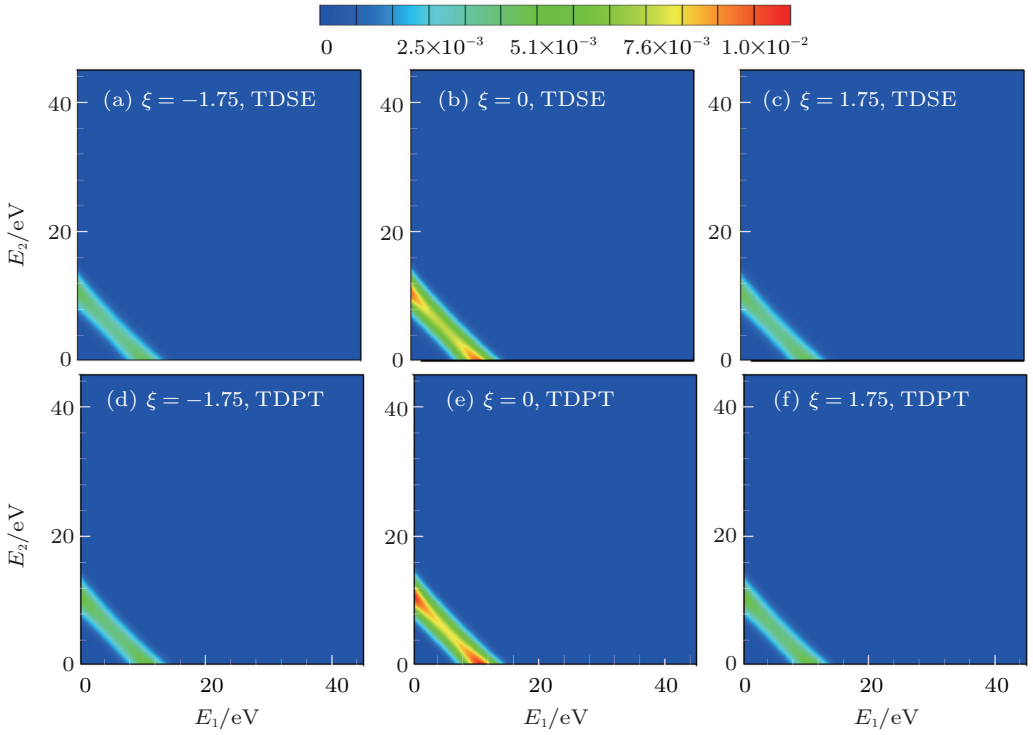


Fig. 3. (color online) Contour plots of the angle-integrated joint energy distribution of both ejected electrons $P(E_1, E_2)$ for $\omega_0 = 45$ eV, at three different chirp parameters: (a), (d) $\xi = -1.75$, (b), (e) $\xi = 0$, and (c), (f) $\xi = 1.75$, respectively, calculated by TDSE (first row) and by TDPT (second row).

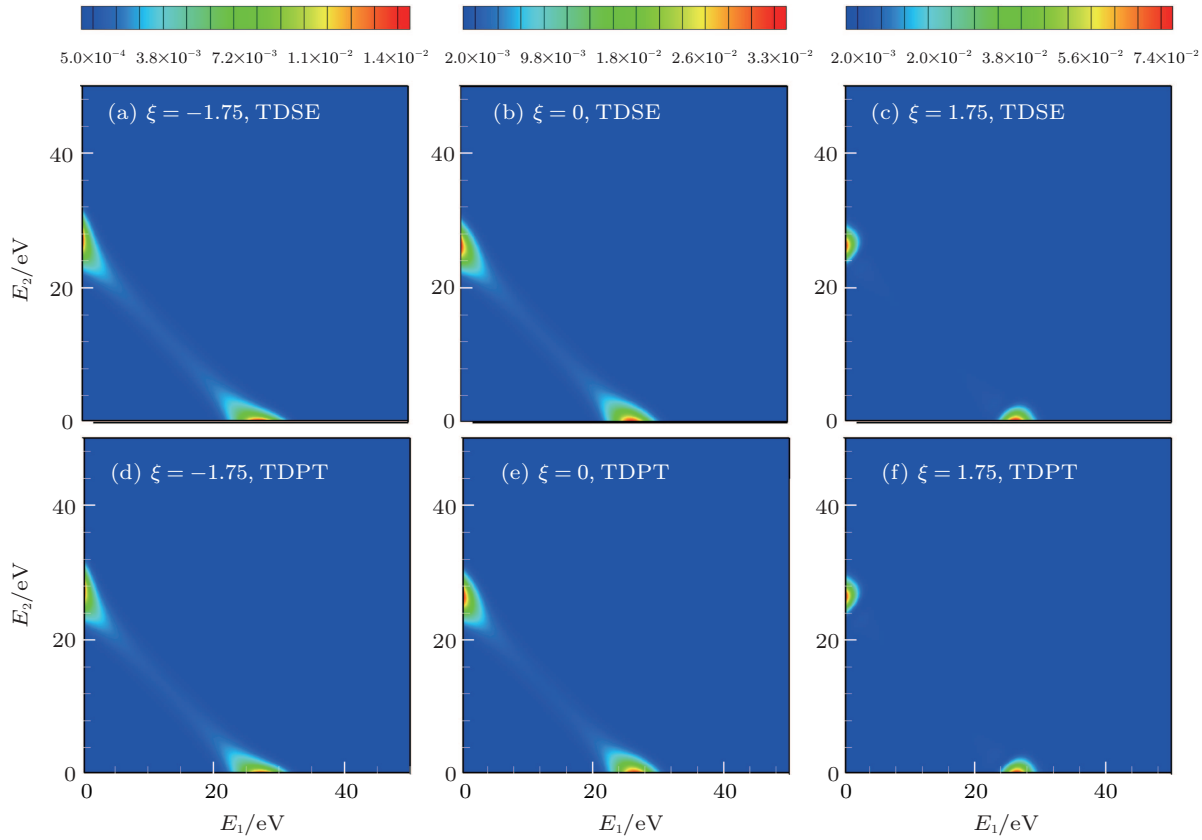


Fig. 4. (color online) Contour plots of the angle-integrated joint energy distribution of both ejected electrons $P(E_1, E_2)$ for $\omega_0 = 52.4$ eV, at three different chirp parameters: (a), (d) $\xi = -1.75$, (b), (e) $\xi = 0$, and (c), (f) $\xi = 1.75$, respectively, calculated by TDSE (first row) and by TDPT (second row).

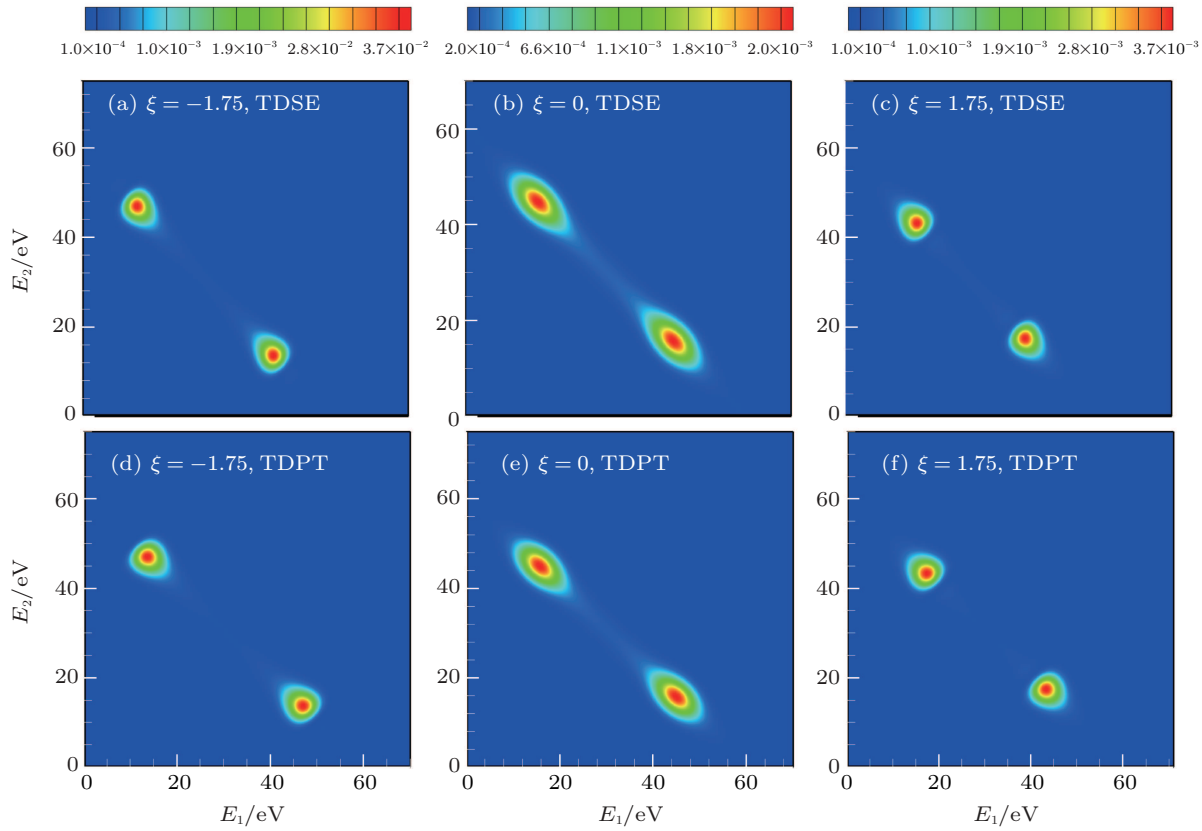


Fig. 5. (color online) Contour plots of the angle-integrated joint energy distribution of both ejected electrons $P(E_1, E_2)$ for $\omega_0 = 70$ eV, at three different chirp parameters: (a), (d) $\xi = -1.75$, (b), (e) $\xi = 0$, and (c), (f) $\xi = 1.75$, respectively, calculated by TDSE (first row) and by TDPT (second row).

It is interesting to check whether $P(E_1,E_2)$ will depend on the chirp parameter, provided that the total yield $P_{\rm total}$ is almost a constant, as shown in Fig. 2(d). We find from Fig. 5 that the joint energy spectra actually change a lot as one changes ξ. In all the cases shown, one mainly sees the sequential peaks, but with different features. The most prominent difference is that, the position of the sequential peak is different for a different chirp parameter. In addition, the detailed shape of each sequential peak is slightly different. For $\xi = 0$ in Fig. 5(b), the sequential peaks look like two quite symmetric ellipses with a clearly equal energy sharing line connecting both of them. For $\xi = -1.75$ in Fig. 5(a), there is also a vaguely visible equal energy sharing line connecting both sequential peaks, which are now asymmetric with the extreme nonequal energy sharing case quickly becoming impossible. For the up-chirped case of $\xi = 1.75$, the pattern shown in Fig. 5(c) is somewhat a reversed case of that in Fig. 5(a): the asymmetric sequential peaks reverse their directions with the equal energy sharing channel that becomes forbidden.

The shift of the position of the sequential peak for a different chirp parameter has been observed previously by Lee *et al.*,[52] at a much larger photon energy of 91.6 eV for different values of positive chirp. These authors did not offer any reasonable explanations, but suspected that the "interferences" between the sequential and the nonsequential channels may be the origin of these structures. Here, by extending the chirp to be a negative value, we find that the energy sharing between the two electrons becomes even unequal. An increased positive chirp will force the two electrons to more equally share the total available net energy.

In order to examine the peaks more clearly, we turn to look at the singly differential ionization probability $\mathrm{d}P/\mathrm{d}E$, which is simply calculated by integrating one of the variables in $P(E_1,E_2)$, say, E_2. The results are shown in Fig. 6 for the three different ω_0 discussed above for different chirp parameter ξ. These panels in Fig. 6 make the phenomena we observe more transparent and intuitive. Here, we want to focus on the case for $\omega_0 = 70$ eV in Fig. 6(c). We find that, the sequential peak shift can be intuitively explained as follows, bearing in mind the deep sequential feature for this ω_0. Let us suppose the first electron gets ionized by absorbing a photon energy of ω_1 to acquire an energy $E_1 = \omega_1 - 24.6$ eV, while the second electron gets an energy of $E_2 = \omega_2 - 54.4$ eV. Then the energy difference is $\Delta E = E_1 - E_2 = (\omega_1 - \omega_2) + 29.8$ eV. This simply tells us that, for the case of $\xi = 0$, at all possible ionization time events, $\omega_1 - \omega_2 = 0$, which gives the usual energy peak separation of 29.8 eV, as shown by the solid line in Fig. 6(c). However, for a negative chirp of -1.75 as shown by the dashed line in Fig. 6(c), the higher frequency component comes first and the lower frequency component comes last. This means that, for most of the ionization sequences time windows, $\omega_1 - \omega_2 > 0$, which will result in an energy spacing larger than 29.8 eV. In a similar fashion, one can explain why, for $\xi = 1.75$, the energy spacing between the sequential peaks is smaller than 29.8 eV, as shown by the dash-dotted curve in Fig. 6(c).

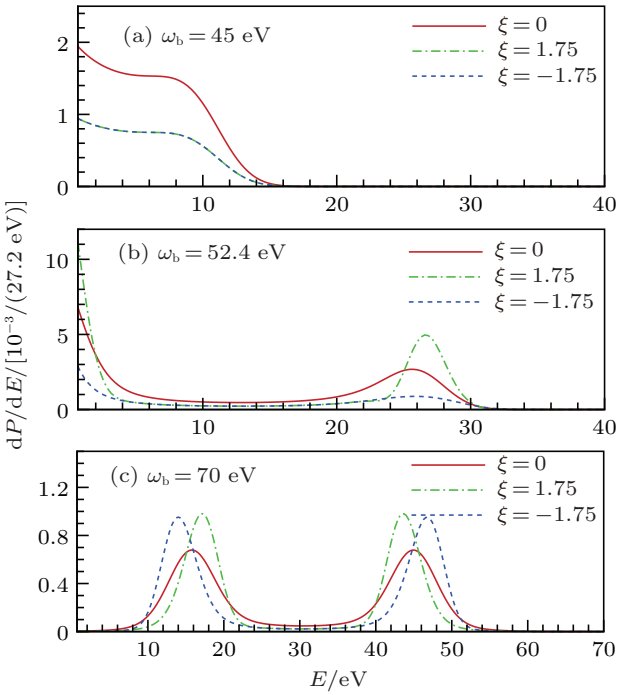


Fig. 6. (color online) Singly differential ionization probabilities $\mathrm{d}P/\mathrm{d}E$, calculated by integrating one of the two variables in $P(E_1,E_2)$, for different central photon energy ω_0: (a) 45 eV, (b) 52.4 eV, and (c) 70 eV. In each panel, the results are shown for three different chirp parameters ξ, i.e., 0 (solid), 1.75 (dash-dotted), and -1.75 (dashed).

4. Conclusions

In conclusion, through two different theoretical methods (TDSE and TDPT), we have systematically studied the chirp dependence of the double ionization process for a wide range of central photon energies, especially in the nonsequential regime which has not been touched before. The model based on TDPT well reproduce the results from numerical TDSE calculations. We have examined the chirp dependence for both the total TPDI yield and the joint energy spectra as well as the singly differential probability. We find, in the nonsequential and translation regions, both the integral and the differential ionization probability depend on the chirp, while for the deep sequential region only the differential signals rely on the chirp parameter with the total double ionization yield almost unchanged. We have provided an intuitive explanation for these chirp-dependent observations.

References

[1] Brabec T and Krausz F 2000 *Rev. Mod. Phys.* **72** 545
[2] Chini M, Zhao K, and Chang Z 2014 *Nat. Photon.* **8** 178
[3] Zewail A 2000 *J. Phys. Chem. A* **104** 5660
[4] Krausz F and Ivanov M 2009 *Rev. Mod. Phys.* **81** 163

[5] Peng L Y, Jiang W C, Geng J W, Xiong W H and Gong Q 2015 *Phys. Rep.* **575** 1
[6] Cheng W J, Zhang S A, Jia T Q, Feng D H and Sun Z R 2014 *Chin. Phys. Lett.* **31** 053301
[7] Zhao X, Yang Y J, Liu X S and Wang B B 2014 *Chin. Phys. Lett.* **31** 043202
[8] Wang C L, Sun R P, Chen Y J, Gong C, Lai X Y, Kang H P, Quan W and Liu X J 2014 *Chin. Phys. Lett.* **31** 063202
[9] Chelkowski S and Bandrauk A D 1997 *Raman Spectrosc. J.* **28** 459
[10] Hornung T, Meier R and Motzkus M 2000 *Chem. Phys. Lett.* **326** 445
[11] Légaré F, Chelkowski S and Bandrauk A D 2000 *Chem. Phys. Lett.* **329** 469
[12] Malinovsky V S and Krause J L 2001 *Eur. Phys. J. D* **14** 147
[13] Sarkar C, Bhattacharya R, Bhattacharyya S S and Saha S 2008 *Phys. Rev. A* **78** 023406
[14] Plenge J, Wirsing A, Raschpichler C, Meyer M and Rühl E 2009 *J. Chem. Phys.* **130** 244313
[15] Marani R and Robinson E J 1999 *J. Phys. B* **32** 711
[16] Chatel B, Degert J, Stock S and Girard B 2003 *Phys. Rev. A* **68** 041402
[17] Djotyan G P, Bakos J S, Sörlei Z S and Szigeti J 2004 *Phys. Rev. A* **70** 063406
[18] Malinovskaya S A 2006 *Phys. Rev. A* **73** 033416
[19] Xiang Y, Niu Y and Gong S 2009 *Phys. Rev. A* **79** 053419
[20] Xu J, Zeng B and Yu Y 2010 *Phys. Rev. A* **82** 053822
[21] Yu C, Sun Z R and Guo D S 2015 *Acta Phys. Sin.* **64** 124207 (in Chinese)
[22] Zhong H Y, Guo J, Zhang H D, Du H and Liu X S 2015 *Chin. Phys. B* **24** 073202
[23] Xia C L and Miao X Y 2015 *Chin. Phys. Lett.* **32** 43202
[24] Ganeev R A, Singhal H, Naik P A, Kulagin I A, Redkin P V, Chakera J A, Tayyab M, Khan R A and Gupta P D 2009 *Phys. Rev. A* **80** 033845
[25] Xiang Y, Niu Y and Gong S 2009 *Phys. Rev. A* **80** 023423
[26] Nakajima T 2007 *Phys. Rev. A* **75** 053409
[27] Nakajima T and Cormier E 2007 *Opt. Lett.* **32** 2879
[28] Abel M J, Pfeifer T, Jullien A, Nagel P M, Bell M J, Neumark D M and Leone S R 2009 *J. Phys. B* **42** 075601
[29] Liu M, Guo Y C and Wang B B 2015 *Chin. Phys. B* **24** 073201
[30] Niu Y, Xiang Y, Qi Y and Gong S 2009 *Phys. Rev. A* **80** 063818
[31] Wright M J, Pechkis J A, Carini J L, Kallush S, Kosloff R and Gould P L 2007 *Phys. Rev. A* **75** 051401
[32] Baltuška A, Udem Th, Uiberacker M, Hentschel M, Goulielmakis E, Gohle Ch, Holzwarth R, Yakovlev V S, Scrinzi A, Hänsch T W and Krausz F 2003 *Nature* **421** 611
[33] Sansone G, Benedetti E, Calegari F, Vozzi C, Avaldi L, Flammini R, Poletto L, Villoresi P, Altucci C, Velotta R, Stagira S, De Silverstri S and Nisoli M 2006 *Science* **314** 443
[34] Goulielmakis E, Schultze M, Hofstetter M, Yakovlev V S, Gagnon J, Uiberacker M, Aquila A L, Gullikson E M, Atwood D T, Kienberger R, Krausz F and Kleineberg U 2008 *Science* **320** 1614
[35] Peng L Y and Starace A F 2007 *Phys. Rev. A* **76** 043401
[36] Peng L Y, Pronin E A and Starace A F 2008 *New J. Phys.* **10** 025030
[37] Ngoko Djiokap J M, Hu S X, Jiang W C, Peng L Y and Starace A F 2012 *New J. Phys.* **14** 095010
[38] Ngoko Djiokap J M, Hu S X, Jiang W C, Peng L Y and Starace A F 2013 *Phys. Rev. A* **88** 011401
[39] Agostini P and DiMauro L F 2004 *Rep. Prog. Phys.* **67** 813
[40] Hofstetter M, Schultze M, Fieβ M, Dennhardt B, Guggenmos A, Gagnon J, Yakovlev V S, Goulielmakis E, Kienberger R, Gullikson E M, Krausz F, and Kleineberg U 2011 *Opt. Express* **19** 1767
[41] Yudin G L, Bandrauk A D and Corkum P B 2006 *Phys. Rev. Lett.* **96** 063002
[42] Yudin G L, Patchkovskii S and Bandrauk A D 2008 *J. Phys. B* **41** 045602
[43] Krasovskii E E and Bonitz M 2009 *Phys. Rev. A* **80** 053421
[44] Peng L Y, Tan F, Gong Q H, Pronin E A and Starace A F 2009 *Phys. Rev. A* **80** 013407
[45] Tan F, Peng L Y and Gong Q H 2009 *Chin. Phys. B* **18** 4807
[46] Pronin E A, Starace A F and Peng L Y 2011 *Phys. Rev. A* **84** 013417
[47] Nabekawa Y, Hasegawa H, Takahashi E J and Midorikawa K 2005 *Phys. Rev. Lett.* **94** 043001
[48] Hasegawa H, Takahashi E J, Nabekawa Y, Ishikawa K L and Midorikawa K 2005 *Phys. Rev. A* **71** 023407
[49] Palacios A, Horner D A, Rescigno T N and McCurdy C W 2010 *J. Phys. B* **43** 194003
[50] Jiang W C, Shan J Y, Gong Q and Peng L Y 2015 *Phys. Rev. Lett.* **115** 153002
[51] Jiang W C, Xiong W H, Geng J W, Gong Q and Peng L Y 2016 *Advances of Atoms and Molecules in Strong Laser Fields*, Ed. Y. Liu, Chapter 5, p. 111 (New Jersey: World Scientific)
[52] Lee T G, Pindzola M S and Robicheaux F 2009 *Phys. Rev. A* **79** 053420
[53] Barmaki S, Lanteigne P and Laulan S 2014 *Phys. Rev. A* **89** 063406
[54] Zhang Z, Peng L Y, Xu M H, Starace A F, Morishita T and Gong Q 2011 *Phys. Rev. A* **84** 043409
[55] Jiang W C, Peng L Y, Xiong W H and Gong Q 2013 *Phys. Rev. A* **88** 023410
[56] Jiang W C, Xiong W H, Zhu T S, Peng L Y and Gong Q 2014 *J. Phys. B* **47** 091001
[57] Laulan S, Ba H S and Barmaki S 2014 *Can. J. Phys.* **92** 194
[58] Palacios A, Rescigno T N and McCurdy C W 2009 *Phys. Rev. Lett.* **103** 253001
[59] Verner D A, Ferlan G J, Korista K T and Yakovlev D G 1996 *Astrophys. J.* **465** 487